MET O 11 TECHNICAL NOTE NO 229

A PARAMETRIZATION OF DEEP CONVECTION FOR USE IN A NON-HYDROSTATIC MESOSCALE MODEL

By

R T H Barnes and B W Golding

Met O 11 (Forecasting Research)
Meteorological Office
London Road
Bracknell
Berkshire RG12 2SZ
ENGLAND

March 1986

A parametrization of deep convection for use in a non-hydrostatic mesoscale model.

By R T H Barnes and B W Golding

Meteorological Office, Bracknell

Summary

The deep convection parametrization scheme used in the UK Meteorological Office mesoscale model is described, and alternative treatments of environmental subsidence effects suggested.

A series of idealized experiments is presented, with (i) no convective parametrization, (ii) subsidence effects parametrized by grid scale warming and drying, and (iii) grid scale subsidence forced by mass sources and sinks due to the parametrized convective updraughts and downdraughts. Numerical problems associated with a crude implementation of (iii) are identified and overcome.

It is found that, (i) fails to produce realistic rainfall amounts or humidity profiles, while (ii), because there is no dynamical adjustment to balance the warming and drying, produces spurious grid scale ascent. In (iii) temperature and humidity changes similar to those in (ii) are produced by the forced grid scale subsidence.

Finally a comparison is made of the behaviour of (ii) and (iii) in a typical synoptic situation, and the small differences in forecast evolution related to the differing grid scale vertical velocity responses.

1. Introduction

The problem of parametrizing sub-grid scale convective motions in numerical weather prediction models has received much attention over the past two decades (Kuo 1974, Arakawa and Schubert 1974, Frank 1983). The majority of these studies have tackled the problem of parametrization for global General Circulation Models with coarse grid meshes and in which the primary requirement is to model the convective fluxes in the tropics which drive the atmospheric general circulation. This problem has not been solved and in recent years has been complicated by the realisation that much tropical convection is organised in mesoscale systems which do not behave merely as a sum of statistically independent clouds. However, with the development of finer mesh regional models, another problem has become apparent. This results from a breakdown in the assumption of a homogeneous, stationary population of clouds within a grid square when the grid length is reduced to a few cloud diameters.

In the UK Meteorological Office mesoscale model (Tapp and White 1976, Carpenter 1979, Golding and Machin 1984) a 15 km grid is currently used. It uses the non-hydrostatic, compressible equations of motion, integrated using a semi-implicit time stepping scheme. Its vertical co-ordinate is height above ground, and in the present version, 16 levels were carried as shown in Table 1. Vertical mixing is determined using a $1^1/_2$ order turbulence scheme based on Yamada and Mellor (1979) and modified

for the presence of moisture following Sommeria and Deardorff (1977). This allows for the diagnosis of sub-grid scale condensation. The condensed moisture is carried as grid scale cloud and a simple parametrization of precipitation from such cloud is employed. The radiative effects of the cloud on the surface heat balance are parametrized in terms of the total liquid water path. The timestep used in the model was one minute.

Very few attempts have been made to parametrize deep convection for models on this scale (Kreitzberg and Perkey 1976, Fritsch and Chappell 1980 (hereafter referred to as FC)). In some special circumstances, eg hurricanes (Rosenthal 1978), it has been found appropriate to allow the explicit representation of convection on a grid scale of up to 10 km. However, numerical cloud models clearly indicate that a grid length of 1-2 km is necessary to resolve the structures of updraughts and downdraughts in individual clouds. As an example, in our own model the onset of showers in the diurnal cycle is poorly represented without a convection scheme because the turbulent mixing produces a layer of low cloud which shields the surface from further radiative heating.

One response to this problem is to average over sufficient model gridlengths to give a suitably large cloud population. However, this is also inadequate because the local response is required both for direct forecasting purposes and to force dynamical responses at these scales.

The alternative has been to follow the approach used in large scale models but to modify it so that the parametrization is more clearly dealing with one cloud or a small number of which a representative one is modelled. Thus FC have a sophisticated steady state representation of a cloud, which lasts for many model timesteps, while Kreitzberg and Perkey (1976) use a time dependent 1-D model. In both these schemes, the direct influence of the cloud is restricted to the grid square in which it is contained. FC are careful to point out that the compensating subsidence occurs only in that part of the grid square not occupied by cloud. Clearly with a 10 km grid this may lead to subsidence velocities of several m s^{-1} if a cloud of 5 km diameter or more is diagnosed.

Another alternative is to use a fully interactive nested cloud model for each cloud or convective area that is diagnosed. Although this removes the difficulties of parametrization, it is expensive and difficult to code in a model. In particular, simplifying assumptions have to be made about overlapping clouds and about growth and decay of convective areas.

In order to find a simpler solution which avoids the constraint of subsidence within the grid square, the scales being represented are reconsidered. The smallest scale is the updraught which typically has a scale of a km or so. This is clearly a sub-grid scale feature and must be parametrized. The downdraught can be considered to be coincident with the rain area

since it is produced by precipitation drag and evaporative cooling. Thus it has a scale of a few km, and should also be parametrized. The subsidence area is seen by the spacing between clouds in a field of convection, and for deep clouds is typically 10 km or more, extending to perhaps 100 km in organised systems. It is not obvious that this should be parametrized in a 15 km mesh model. The subject of this paper is therefore to consider whether a parametrization of the updraught and downdraught alone can produce a viable representation of deep convection in a mesoscale model. Clearly such a parametrization will involve mass sources and sinks. In a hydrostatic model these would simply lead to an instantaneous vertical adjustment in the model column concerned which would be entirely consistent with the normal parametrization of local subsidence. However, in a non-hydrostatic model, such as that used here, the vertical redistribution will occur through the development of a vertical acceleration supported by appropriate pressure adjustments. It is reasonable to suppose that this will not be confined to the grid square containing the cloud, and may occur in a realistic manner.

In section 2 the outline of the full parametrization scheme, derived from FC, is given. Section 3 describes in detail the formulation of the mass sources and sinks in the mesoscale model equations. The results of the new scheme are compared with other solutions for an idealised cloud in section 4 and the response of the full model in a real situation is shown in section 5. Finally

some weaknesses in the scheme as a whole are aired in section 6 together with suggestions for work needed to further validate the scheme.

2. Outline of the scheme

The parametrization scheme is based closely on that described by Fritsch and Chappell (1980) the main difference being in the downdraught which they parametrized to represent the processes in a continental severe storm. An early version has been described in Golding (1983). As in FC, each cloud is assumed to last for several model timesteps. In the present scheme, the cloud base characteristics and cloud depth are stored and the resulting increments recalculated each timestep. The structure of the scheme is described under the headings: location and duration of clouds, updraught, rainfall, downdraught and grid scale effects. The latter includes the parametrization of subsidence, replacement of which is the main concern of this paper. Figure 1 shows a schematic representation of these processes.

(a) Location and duration of clouds

It has been found that free convection in the boundary layer is adequately treated by the model's turbulent diffusion parametrization until saturation occurs, ie it is the release of potential instability that has to be parametrized. Diagnosis of an unstable grid volume requires, therefore, that it contain

cloud (at least 10% cover), that the large scale vertical motion is upwards and that the volume is upwardly buoyant when lifted to the next model level after account is taken of latent heat release. Only grid volumes between 500 m and 4000 m above ground level are tested.

Having located an unstable volume, cloud top is determined by lifting with entrainment until it is no longer buoyant. This is an iterative process since the entrainment coefficient is defined (as in FC) so as to double the mass flux through the cloud depth. Any cloud diagnosed as having a depth of under 2000 m is discarded (this is necessary for computational reasons but such clouds are more appropriately handled by the turbulent diffusion parametrization anyway).

Each cloud lasts for one hour but grid volumes are tested every 15 min so in principle a new cloud could be diagnosed that often. Clouds are advected at the speed of their mid-level wind, the increments being assigned to the nearest grid point.

(b) Updraught structure

The mass flux of the updraught M_u is computed so that the resulting subsidence will increase the temperature of the environment to that of the updraught at all levels in the cloud in the absence of other processes. Thus

$$M_u(k) = 2(T_u(k) - T_{env}(k))/(T_{env}(k+1) - T_{env}(k-1))M_g(k) \quad kg\ hr^{-1}$$

at each level k, where M_g is the grid-box mass, T_u is the updraught temperature and T_{env} is the environment temperature.

Given a linear increase of M_u from cloud base to top, the necessary cloud base mass flux $M_u(CB)$ can then be defined which will satisfy the above equation for each level and the largest value is used. Under certain circumstances, a tall cloud with a small mass flux might be diagnosed. This is physically unrealistic so a standard unit of cloud base mass flux of 10^{11} (H/8000) kg hr^{-1} is defined for a cloud of depth H and the actual $M_u(CB)$ is made an integer multiple of this.

The updraught characteristics are computed by progressively adding environment air to the original cloud base values thus

$$T_u(k+1) = (M_u(k)T_u(k) + (M_u(k+1)-M_u(k))T_{env}(k))/M_u(k+1)$$

where $$M_u(k) = M_u(CB)(1+ \Delta z(k)/H)$$

This calculation is performed for temperature, humidity and wind, the first two being mutually adjusted at each level to remove condensed vapour which is accumulated up to cloud top. At cloud top, the outflow is the same temperature as the environment but increments of humidity and wind are calculated. Mixing at lower levels is defined so that the instantaneous mass in the updraught column is mixed into the environment over the cloud's lifetime. This simulates the dissipation process and depends on an

updraught area A_u being defined. Rather than computing this via the mass flux and updraught velocity, which produces doubtful results on occasions, a fixed value is defined from the cloud base mass flux:

$$A_u = M_u(CB)/(3600\ w_u(CB))$$

where $w_u(CB) = 2\ ms^{-1}$

(c) Rainfall

The rainfall is calculated by applying an efficiency factor E to the total condensate accumulated in the updraught. This depends on the shear and ambient humidity at cloud levels and on the ambient humidity below cloud base. Thus

$$E = E_o - E_1 \left|\frac{\Delta \underline{u}}{\overline{\overline{H}}}\right| (1 - \overline{\overline{RH}}^{cloud}) + E_2 t (\overline{\overline{RH}}^{sub\text{-}cloud} - RH_o)$$

where $E_o = 0.5$, $E_1 = 100$, $E_2 = 2 \times 10^{-5}$, $RH_o = 80\%$, $t = 0.2$.

The latter parameter is an estimate of the proportional weighting of downdraught and ambient air in the sub-cloud layer as the rain falls through it, evaporation at the standard humidity RH_o being included in E_o.

It is necessary to estimate the area over which rain falls from the cloud since this defines the downdraught area and also the average rainfall intensity in the shower. This departs from FC

where a parcel calculation of downdraught mass flux is used. The estimation of area starts from a linear relation with cloud depth based on crude assumptions about aspect ratio. This is expressed in terms of the cloud base mass flux and is then modified to enlarge the area as the shear increases. Thus

$$A_R = \frac{M_u}{M_o}(CB)\left(1 + a\left|\frac{\Delta \underline{u}}{H}\right|\right) \qquad \text{where } a = 100 \text{ and } M_o = 3600$$

The non-precipitated condensate is partitioned into 3 parts: evaporation below cloud base (see below), mixing into the environment in the lower part of the cloud, and mixing into the environment in the upper part of the cloud. The last two are calculated in the proportion 40% to lower levels and 60% to upper levels.

(d) Downdraught structure

The penetrative downdraught structure used in FC is not a characteristic of UK maritime cumulonimbus clouds. However, the cold outflow from the downdraught is still important in the near surface meteorology. Further ad hoc assumptions about its nature have therefore been made to simplify the calculation. The area is assumed to be the rain area calculated above and the mass flux up to cloud base is set to

$M_d = \rho z_{CB} A_R$ kg hr^{-1}, where z_{CB} is cloud base height and ρ is the density.

Above cloud base the area remains constant but the mass flux decreases linearly to half its cloud base value at the cloud's middle level where it is assumed to originate. The properties of the downdraught are assumed equal to the updraught above cloud base. In the sub-cloud layer it descends adiabatically but with a modification in the outflow due to evaporation. This is assumed to be

$$\Delta q = Q_o(1-RH_o - t(\overline{RH}^{\text{sub-cloud}} - RH_o))\, P^{0.5} M_d \text{ kg } hr^{-1}$$

where $Q_o = 0.0072$, RH_o and t are as before, and P is the local precipitation rate. The modified outflow air is mixed into the model's lowest three layers. At other levels, as with the

updraught, dissipation is modelled by mixing the instantaneous mass of downdraught air into the environment during the lifetime of the cloud.

(e) Grid scale effects

In the updraught section fluxes at cloud top due to the outflow and at cloud levels modelling dissipation were described. In the rainfall section, fluxes of non-precipitated condensate were calculated. In the downdraught section, fluxes in the lowest three layers due to outflow and at other levels up to the middle of the cloud modelling dissipation were described. The dominant effect on the environment, however, is its response to the fluxes of mass involved in the updraught and downdraught. The principal response is subsidence at cloud levels to compensate for the updraught mass flux (the downdraught being much weaker). In the original implementation this was calculated as in FC by assuming that the remaining mass in each grid volume (after subtracting the updraught and downdraught) must subside sufficiently to compensate. The resultant warming and drying is calculated and applied as a parametrization of the subsidence at each level. As will be seen in section 4, the unfortunate result of this warming is to create a hydrostatic imbalance with the pressure field which is adjusted by upward motion - thus undoing the parametrized warming. This is because the dynamical changes which must accompany subsidence have not been made. Another deficiency of this technique is that as the grid size decreases,

the local heating due to the subsidence becomes greater because of the requirement that all of the compensation should occur in a single grid square. Observational evidence for the effect of the subsidence is indirect but suggests it to be weak and covering a large area. The next section therefore proposes a solution in which the mass imbalances created by the convection are treated as source terms in the grid scale equations, and they compute the necessary response directly, spreading it over several grid squares if necessary.

3. The model equations with mass sources and sinks

The analysis of Tapp and White (1976), hereafter TW, is followed with the addition of the source/sink terms. Given a source of mass M kg s^{-1} within a volume V, the continuity equation becomes

$$\frac{\partial \rho}{\partial t} + \underline{v}.\nabla\rho + \rho\nabla.\underline{v} = \dot{M}/V$$

Eliminating the density ρ, using Exner pressure $\pi = (p/p_s)^{\kappa}$ where p is pressure, p_s = 1000 mb and $\kappa = R/c_p$, and potential temperature θ gives

$$(c_p/R\gamma\pi)\frac{\partial \pi}{\partial t} - \frac{1}{\theta}\frac{\partial \theta}{\partial t} + (c_p/R\gamma\pi)\ \underline{v}.\nabla\pi - \frac{1}{\theta}\underline{v}.\nabla\theta + \nabla.\underline{v} = \dot{M}/\rho V$$

where $\gamma = c_p/c_v$ and using $c_p = (1-\kappa)/\kappa = c_p/R\gamma$.

Substituting from the thermodynamic equation

$$\frac{\partial\theta}{\partial t} + \underline{v}.\nabla\theta = \frac{\dot{Q}\theta}{c_p T}$$

where $\dot{Q}$ represents sources/sinks of heat, writing $\rho V = M$, the mass of the grid volume, $c^2 = \gamma RT$, the speed of sound, and using $R\gamma/c_p = \gamma - 1$, gives

$$c_p\theta\left[\frac{\partial\pi}{\partial t} + \underline{v}.\nabla\pi\right] + c^2\,\nabla.v = (\gamma-1)\dot{Q} + \frac{c^2}{M}\dot{M}$$

Comparing with the corresponding equation in TW, we see that the effect of the mass sources sinks has been the addition of the

extra term, $c^2\dot{M}/M$. Following TW, we introduce $\theta = \theta_o+\theta_1$ and $\pi = \pi_o+\pi_1$, where $\pi_o = 1-gz/c_p\theta_o$ is the hydrostatic Exner pressure of the basic state temperature profile. Some manipulation then yields

$$c_p\theta_o\frac{\partial\pi_1}{\partial t} - gw - c_o^2\nabla.v = -c_p\theta_o\left[\underline{v}.\nabla\pi_1 + (\gamma-1)\pi_1\nabla.\underline{v} - \frac{(\gamma-1)\dot{Q}}{c_p(\theta_o+\theta_1)} - \frac{\dot{M}}{M}\left(\frac{c_o^2}{c_p\theta_o} + (\gamma-1)\pi_1\right)\right]$$

where $c_o^2 = \gamma R\theta_o P_o$ is the basic state speed of sound. Manipulation of this and the other model equations in finite difference form as in TW yields a Helmholtz equation in $c_p\theta_o[\pi_1^{n+1} - 2\pi_1^n + \pi_1^{n-1}]$, the superscripts indicating time levels. An additional term is then needed on the right hand side of this equation of the form

$$(2c_p/c_o^2\Delta t)\left[-\frac{\dot{M}}{M}(c_o^2/c_p\theta_o + (\gamma-1)\pi_1)\right]$$

which may be simplified to

$$(2/\theta_o\Delta t)\left[-\frac{\dot{M}}{M}(\pi_o+\pi_1)/\pi_o\right]$$

The origin of the mass increments was described above in section 2. They may be summarised into two groups, those related to the updraught and those related to the downdraught. Updraught increments are dominated by a sink at cloud base and a source at cloud top with additional small mass sinks at all intermediate levels. For the downdraught, the sink is largest at the cloud's middle level with smaller contributions from the levels in the lower half of the cloud and the source is at the model's lowest level, 10 m above ground level. In general we may write

$$\left(\frac{\dot{M}}{M}\right)_k = (M_u(k)-M_u(k+1) + M_d(k+1) - M_d(k))/\ 3600\ M_k$$

where the factor of 3600 appears because the updraught and downdraught fluxes M_u, M_d are expressed in kg hr^{-1}. M_k is the mass of the grid box at model level k. At level 1, $M_d(k)$ is taken as zero.

As described in section 2 the parametrization yields almost equal increments throughout the cloud's lifetime. Early experiments confirmed that if the mass increments were applied in this way the model would suffer a severe shock as each cloud started or stopped. The resulting four-timestep oscillations are illustrated in Fig. 7. This problem is avoided by scaling the increments so that the mass flux increases linearly over the first quarter of the cloud's life, is constant for the next 30 min and decreases linearly after that. The total mass flux over

the whole hour remains unchanged. The other fluxes were not scaled in this way though it might be appropriate to do so.

A similar problem arose when the influence of a mature cloud moved from one grid point to the next because of the advection scheme. This was avoided by specifying a gridlength square about the notional position of the cloud and assigning proportionate parts of the mass increments to the four surrounding grid squares according to their overlap with the cloud's grid square. By this means the increments change smoothly as the cloud moves across the grid.

4. Experiments with the scheme

In order to test the scheme independently of particular weather patterns, several short forecasts were made from simple initial conditions using a version of the UK Meteorological Office mesoscale model (Tapp and White 1976, Carpenter 1979 and Golding and Machin 1984) with the usual 15 km grid but with a reduced domain of 39 grid points square.

The initial data for the experiments were horizontally uniform with zero velocity. The thermodynamic structure was taken from the ICAO standard atmosphere as shown in Table 1. Values of the relative humidity were chosen to ensure that cloud would form at an appropriate height for convection to be initiated, while initial cloud water was zero everywhere. The ground was taken to

be flat and suitable surface and soil temperatures were specified. At the central point of the grid, short wave heating appropriate to tropical latitudes was specified while at other points no heating was applied. With this strong forcing, convection is diagnosed at the central point on the second pass through the testing routine after 30 minutes of integration. After this, the surface temperature contrast falls due to the effect of the cloud on the diagnosed incoming radiation. The convective cloud formed in this way was of largish size having a cloud base mass flux of 1.75×10^{11} kg hr^{-1} (see section 2.b). The area of the cloud was diagnosed as 49 km^2 which is 22% of the grid square with cloud base at level 4 (610 m) and top at level 11 (5510 m). Table 2 lists the cloud characteristics including the vertical velocity needed to balance the updraught and downdraught as used in the old version of the scheme where the parametrization includes this process. The last two columns refer to specific integrations and will be referred to later.

Integrations were performed:

(i) without a convection scheme;

(ii) with the scheme described in section 2 including parametrization of the compensating vertical motions;

(iii) with the grid scale subsidence scheme described in section 3;

(iv) as (iii) but with smooth time variation of mass increments;

(v) as (iv) but with smooth variation of mass increments as clouds move.

In the first integration, the convection scheme was not called so the the surface heating was communicated to the atmosphere by a grid scale circulation and by the turbulent diffusion parametrization. The latter scheme neutralised the instability once saturation occurred by level-to-level mixing, producing a shallow development of cloud (Fig 2). The grid scale vertical velocities reached a few cm s^{-1}, growing very slowly. The potential for growth of deep clouds in the specified environment was not realised and so the predicted cloud, precipitation, etc are unrealistic.

The second integration used the scheme described in section 2 in which all processes, including compensating vertical motions, were parametrized. The character of the diagnosed cloud is shown in Table 2. The heat increment, resulting from parametrization of the subsidence, gives a hydrostatically unbalanced vertical structure which the model attempts to adjust to by lifting the heated layers. The resulting grid scale vertical velocity structure is shown in Fig 4 after half the cloud's lifetime, and the values are listed under "W_{old}" in Table 2. Maximum upward velocities of 0.31 m s^{-1} are produced at level 9 effectively counteracting a substantial part of the parametrized subsidence. This is an undesirable impact on the grid scale flow since the lifting will lead to destabilization. Development of the circulation can be traced in Fig 5 at 4 levels in the vertical

and the moisture structure is shown in Fig 6. Note the substantial moistening near the top of the cloud where the detrainment of cloud is occurring.

In the remaining integrations, the form of the continuity equation derived in section 3 was used in place of the parametrized vertical motion. Fig 7 shows the response of the model when the full mass increments are applied as soon as the cloud is diagnosed. The shock results in an overshoot in the subsidence velocity followed by a damped oscillation whose amplitude and frequency is largely governed by the time smoothing in the model. After recovery from the shock, the pattern of vertical motion is as shown in Fig 8 with most of the response in the convecting grid square but a small amount of subsidence in surrounding squares. The shock recurs when the mass increments are removed at the end of the cloud's lifetime.

As described in section 3, the shock can be prevented by applying a ramped time distribution of the mass increments. Fig 9 shows that this successfully removes the overshoot and oscillation. The increments during the central part of the cloud's life are larger in this scheme to make up for the smaller increments in the tails, so a somewhat greater steady response is seen. Fig 10 shows this reponse when the cloud is 30 min old and the profile of vertical velocities is shown in the final column of Table 2, "W_{new}". The subsidence is comparable in magnitude with the net effect of the parametrized subsidence, "W", and the

grid scale response, "W_{old}", in the second integration. The subsidence is most marked near cloud top and becomes very weak in the middle of the cloud where it seems to propagate outwards as the cloud matures. Below cloud upward motion of 5 cm s^{-1} is forced from the mass source at the ground and the sink at cloud base. Fig 11 shows the moisture structure at the same time and is very similar to that shown in Fig 6 for the scheme with parametrized subsidence.. The time dependent behaviour of the relative humidity at several model levels is shown in Fig 12.

The final integration shows the use of the grid point sharing scheme for the mass increments when clouds move across the grid. To avoid changing the initial state, the clouds were artifically moved due north at 5 m s^{-1}. Fig 13 shows the time history of vertical velocities near cloud top for the initiating grid point and for the one immediately north of it. As before a cloud is triggered at 30 min. As the cloud moves during its growth stage, parts of the increments are applied at the next grid point giving smaller subsidence velocities of 0.45 m s^{-1} as against 0.58 m s^{-1} (see Fig 9). By timestep 55 the cloud is midway between the two grid points and roughly equal subsidence of 0.23 m s^{-1} is seen at each. Thereafter subsidence decreases at the original grid point until timestep 75 when a new larger cloud is triggered there. At the adjacent grid point subsidence grows as the, now mature, cloud approaches and then decreases as it decays.

5. Response of the full model

Two forecasts have been run using the full mesoscale model on the standard 15 km resolution British Isles grid, with a data time of 06 GMT 21 January 1986. The sole difference between the two forecasts was in the treatment of the environmental subsidence term in the deep convection scheme. One run had subsidence effects parametrized, the other used the mass increments scheme to force subsidence on the grid scale.

At 06 GMT a cold front lay just west of a line from the Wash to the Isle of Wight, with rain reported at all nearby stations. Behind the front was a strong westerly flow with considerable shower activity, including a trough oriented NE-SW approaching the west coasts of Scotland and Ireland.

No attempt is made, of course, to forecast the timing of individual showers at particular grid points, but the model should be able to give indications of regions likely to get showers, their intensity and frequency.

As one would hope the two forecasts show broadly similar evolution, with the frontal rainband leaving SE England and extensive shower activity over the sea and windward coasts.

However by 09 GMT some detailed differences between the forecasts are worth noting. The forecast using the grid scale adjustment (Fig 14) has maintained embedded convection along most of the frontal rainband, while the forecast with parametrized subsidence (Fig 15) has lost the embedded convection over East Anglia. The showery activity associated with the trough in the North West is somewhat more organized in Fig. 14 than in Fig 13. The development of showers west of Cornwall seems to be occurring in slightly different locations between the two forecasts, but with similar intensities and numbers. This last difference is thought to be due to the feedback of the forced vertical velocities on the model dynamics. When subsidence is parametrized, the induced upward motion at convecting grid points promotes further convection at these points, whereas forced grid scale subsidence may suppress further convection there. However, with grid scale adjustment, further convection is encouraged at adjacent grid points in the case of existing isolated showers, and in adjacent regions when most grid points in a region are convecting.

It is difficult to verify these differences of detail with the available observations but the experiment indicates that the grid scale mass adjustment scheme can be used in the full model without instabilities developing.

6. Conclusions

A parametrization of sub-grid scale deep convection has been proposed for mesoscale models. The parametrization deals with the convective scale updraught and downdraught in a similar way to other schemes, in particular that of Fritsch and Chappell (1980). However, noting the larger scale of the compensating subsidence around the cloud, and taking advantage of the non-hydrostatic formulation of the UK Meteorological Office mesoscale model, it was proposed that the mass compensation could be accomplished through the grid scale dynamics. Comparative tests of parametrized and grid scale mass compensation show that the two methods produce comparable amounts of net subsidence. However, while the grid scale scheme leads to the expected grid scale subsidence, the response to parametrized subsidence is grid scale ascent. A result of this difference is that there is a positive feedback towards producing organised convective systems in the parametrized scheme whereas the feedback is mainly negative in the grid scale scheme. In the case study, the initial occurrence of convection was controlled by the large scale initial conditions and the differences between the schemes showed as minor rearrangements of the convecting grid squares rather than major forecast differences. It is to be expected, however, that on some occasions the forecasts may be quite different after several hours' forecast.

The proposed scheme does not solve all of the difficulties associated with parametrizing convection in this sort of model. The model dynamics does not deal well with small scale forcing exciting two gridlength waves which are only damped by the artificial diffusion. It is also noticeable that the response to the mass forcing does not spread significantly beyond the grid square in which the forcing occurs. This suggests that the observed scale may relate to geostrophic rather than hydrostatic adjustment processes. Nevertheless it is suggested that the response is more realistic than that obtained with parametrized subsidence.

List of figures

Fig. 9 Integration 4: scaled mass increments. Graph of vertical velocity for heated grid point.

Fig. 10 Integration 4: scaled mass increments. Cross-section of vertical velocity in cm s^{-1} after 60 min.

Fig. 11 Integration 4: scaled mass increments. Cross-section of relative humidity in % after 60 min.

Fig. 12 Integration 4: scaled mass increments. Graph of relative humidity for heated grid point.

Fig. 13 Integration 5: advection of clouds. Graph of vertical velocity for heated grid point and adjacent grid point to the north at model level 11.

Fig. 14 3-hour forecast from data time 06 GMT 21 January 1986 with subsidence effects of convection forced by mass increments, showing wind feathers, convective precipitation (∇), stratiform precipitation (o - light; o - moderate/heavy).

Fig. 15 As Fig 14, but with subsidence effects parametrized.

Table headings

Table 1 Initial data for idealized experiments. Values of pressure, potential temperature, temperature and relative humidity at each model level.

Table 2 Layer thickness (m), updraught and downdraught mass fluxes M_u, M_d (10^{10} kg hr^{-1}), grid box mass M_g (10^{10} kg), and vertical velocities (m s^{-1}), (i) implied grid scale compensation W, (ii) parametrized subsidence W_{old}, (iii) forced subsidence W_{new}, for a typical model cloud at several levels.

Table 1

Level	Height(m)	P(mb)	θ(°C)	T(°C)	RH(%)
16	12010	192.3	93.5	-44.2	30.0
15	10510	244.1	69.4	-44.2	30.0
14	9110	302.2	49.1	-44.2	30.0
13	7810	365.6	43.3	-35.8	40.0
12	6610	443.4	38.2	-28.0	50.0
11	5510	504.1	33.7	-20.8	60.0
10	4510	576.3	29.8	-14.3	70.0
9	3610	648.2	26.4	-8.5	75.0
8	2810	718.0	23.5	-3.3	80.0
7	2110	784.0	21.0	1.3	85.0
6	1510	844.4	19.0	5.2	90.0
5	1010	897.5	17.3	8.4	94.0
4	610	942.0	15.9	11.0	96.3
3	310	976.5	14.9	13.0	94.0
2	110	1000.0	14.3	14.3	90.0
1	10	1012.0	14.0	14.9	85.0
surface	0	1013.2		14.0	
ground				14.9	

Table 2

Level	Layer Thickness	M_u	M_d	M_g	W	W_{old}	W_{new}
12	1150	0		16.0	-	-0.09	0.09
11	1050	35.0		16.5	-0.79	0.06	-0.45
10	950	31.4		16.6	-0.64	0.26	-0.21
9	850	28.2		16.3	-0.52	0.31	-0.09
8	750	25.4		15.6	-0.43	0.29	-0.05
7	650	22.9	1.5	14.5	-0.34	0.23	-0.04
6	550	20.7	2.0	13.1	-0.28	0.16	-0.07
5	450	18.9	2.5	11.2	-0.23	0.10	-0.10
4	350	17.5	3.0	9.1	-0.20	0.06	-0.11
3	250	0	3.0	6.7	0.04	0.03	0.08
2	150	0	3.0	4.1	0.04	0.01	0.05
1	60	0	0	1.6	-	-	-

References

Arakawa, A and Schubert, W H 1974 Interaction of a cumulus cloud ensemble with the large-scale environment. Part I. J.Atmos.Sci., 31, 674-701.

Carpenter, K M 1979 An experiment using a non-hydrostatic mesoscale model. Quart.J.R.Met. Soc., 105, 629-655.

Frank, W M 1983 The cumulus parameterization problem. (Review). Mon.Weath.Rev., 111, 1859-1871.

Fritsch, J M and Chappell, C F 1980 Numerical prediction of convectively driven pressure systems. Part I: Convective parameterization. J.Atmos.Sci., 37, 1722-1733.

Golding, B W 1983 'Impact of convection schemes on mesoscale models', in ECMWF Workshop on convection in large-scale numerical models. 213-229.

Golding, B W and Machin, N A 1984 The United Kingdom Meteorological Office mesoscale forecasting system. Proc. Nowcasting-II Symposium, Norrkoping, Sweden, 3-7 Sept, 1984 (ESA SP-208), 309-314.

Kreitzberg, C W and Perkey, D J 1976 Release of potential instability: Part I. A sequential plume model within a hydrostatic primitive equation model. J.Atmos.Sci., 33, 456-475.

Kuo, H L 1974 Further studies of the parameterization of the influence of cumulus convection on large-scale flow. J.Atmos.Sci., 31, 1232-1240.

Rosenthal, S L 1978 Numerical simulation of tropical cyclone development with latent heat release by the resolvable scales,I: Model description and preliminary results. J.Atmos.Sci.,35, 258-271.

Sommeria, G and Deardorff, J W 1977 Subgrid-scale condensation in models of non-precipitating clouds. J.Atmos.Sci., 34, 344-355.

Tapp, M C and White, P W 1976 A non-hydrostatic mesoscale model. Quart.J.R.Met.Soc., 102, 277-296.

Yamada, T and Mellor, G L 1979 A numerical simulation of BOMEX data using a turbulence closure model coupled with ensemble cloud relations. Quart.J.R.Met.Soc., 105, 915-944.

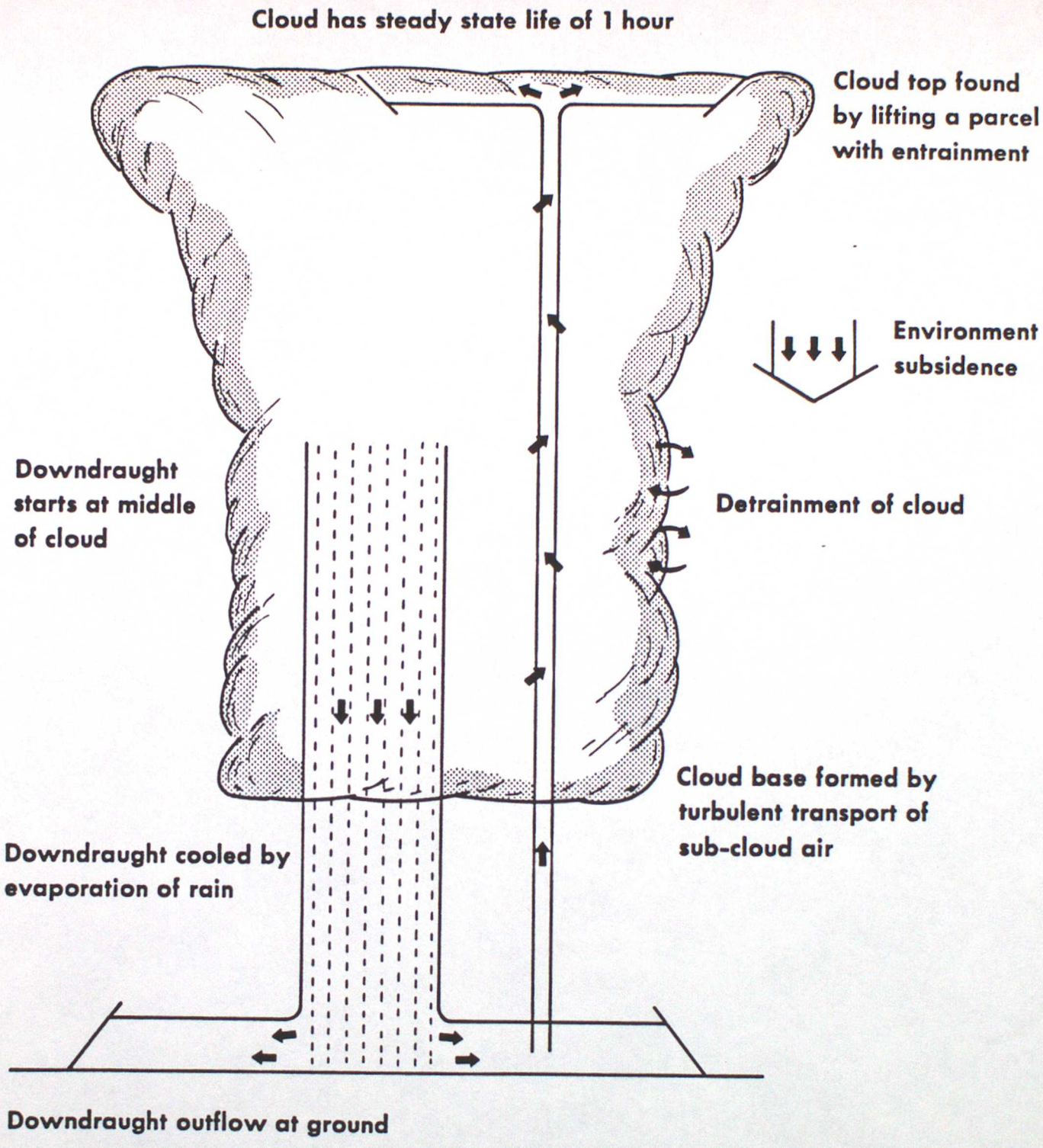
Cloud has steady state life of 1 hour
Cloud top found by lifting a parcel with entrainment
Environment subsidence
Downdraught starts at middle of cloud
Detrainment of cloud
Cloud base formed by turbulent transport of sub-cloud air
Downdraught cooled by evaporation of rain
Downdraught outflow at ground

Fig. 1

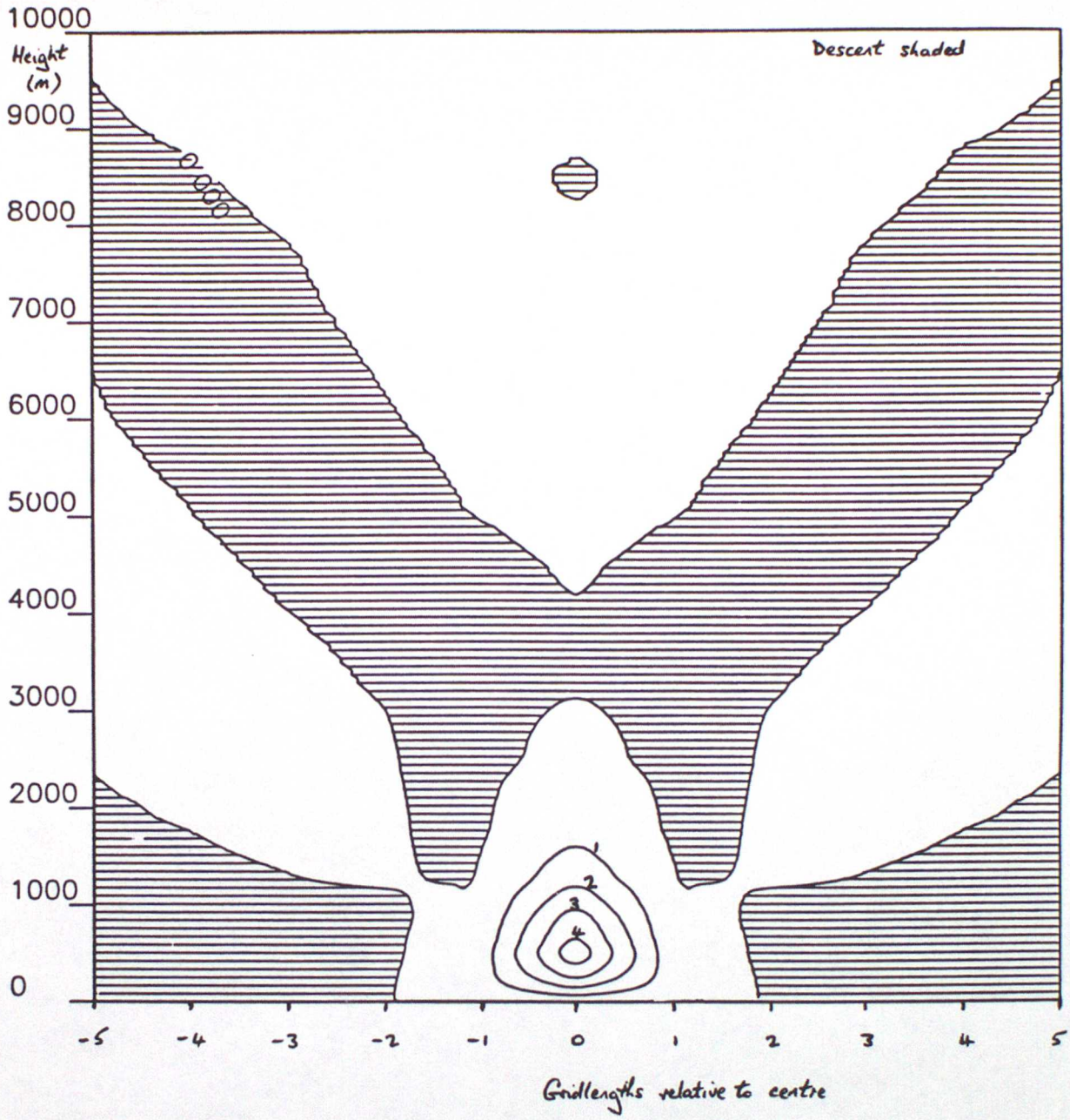
10000
Height (m)
9000
8000
7000
6000
5000
4000
3000
2000
1000
0
Descent shaded
1
2
3
4
-5
-4
-3
-2
-1
0
1
2
3
4
5
Gridlengths relative to centre

Fig 2

FIG.3

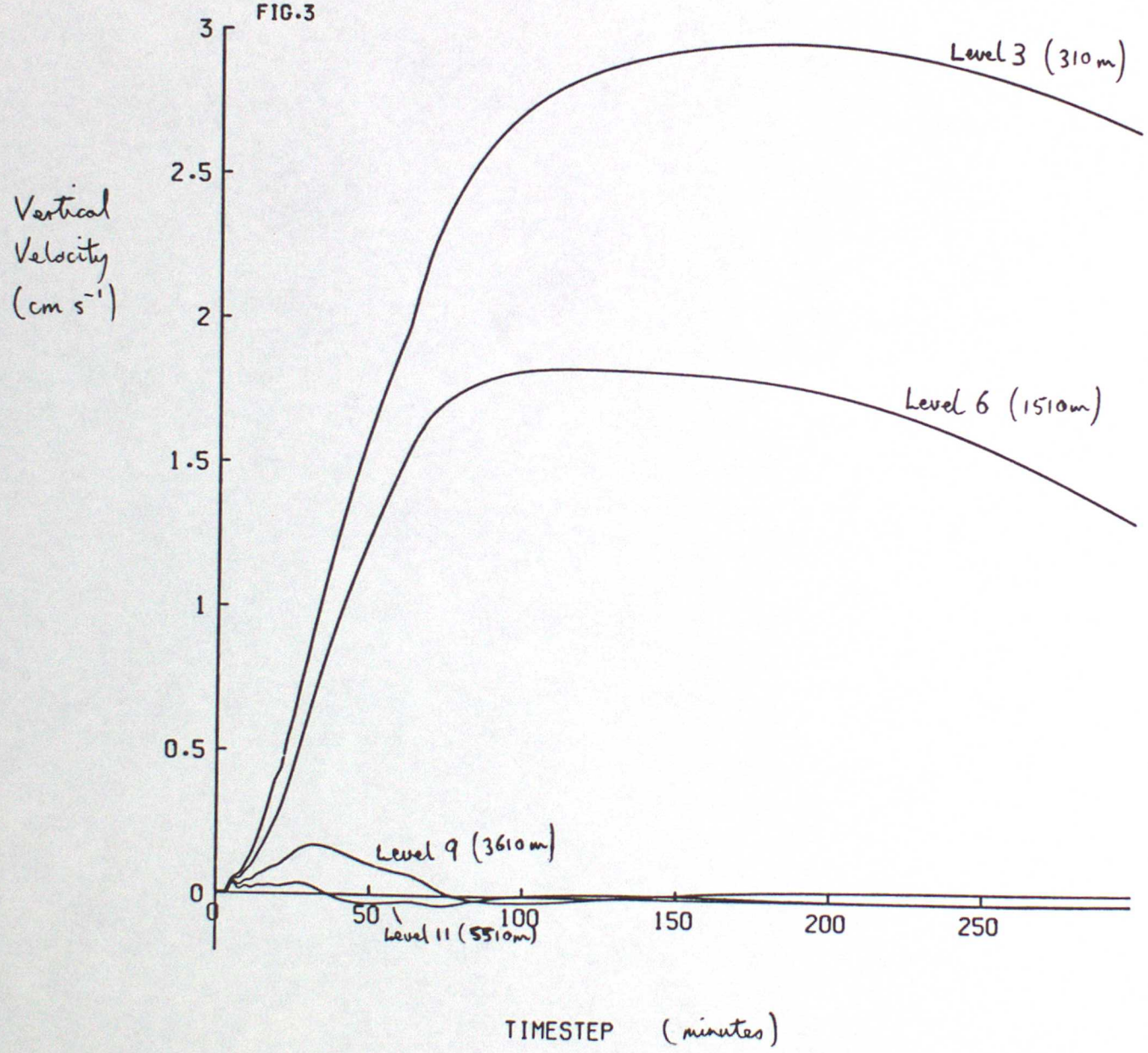
Vertical Velocity (cm s⁻¹)
3
2.5
2
1.5
1
0.5
0
0
50
100
150
200
250
Level 3 (310 m)
Level 6 (1510m)
Level 9 (3610 m)
Level 11 (5510m)
TIMESTEP (minutes)

Fig. 3.

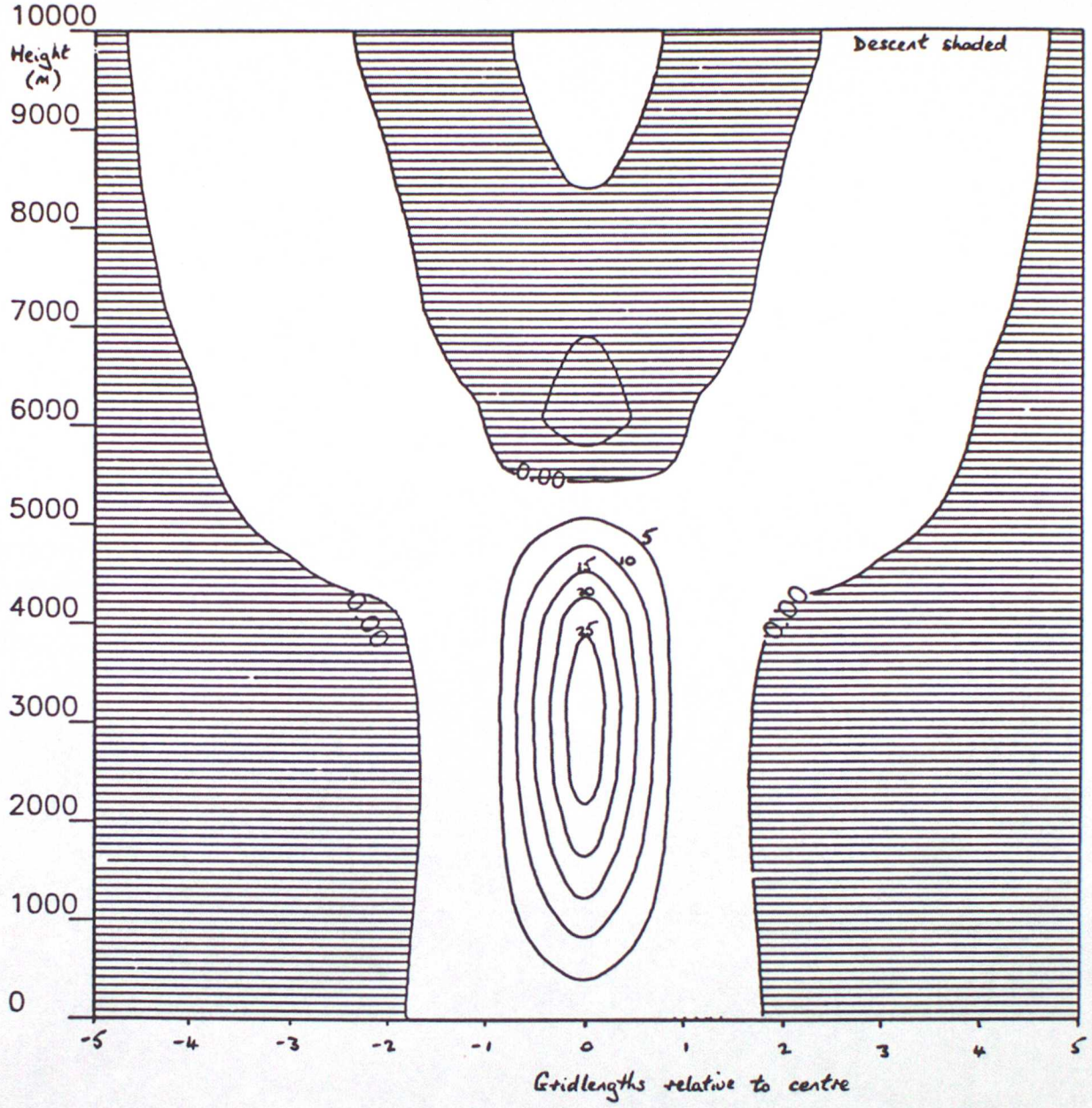
10000
Height (m)
9000
8000
7000
6000
5000
4000
3000
2000
1000
0
Descent shaded
0.00
0.00
0.00
5
10
15
20
25
-5
-4
-3
-2
-1
0
1
2
3
4
5
Gridlengths relative to centre

Fig. 4

FIG.5

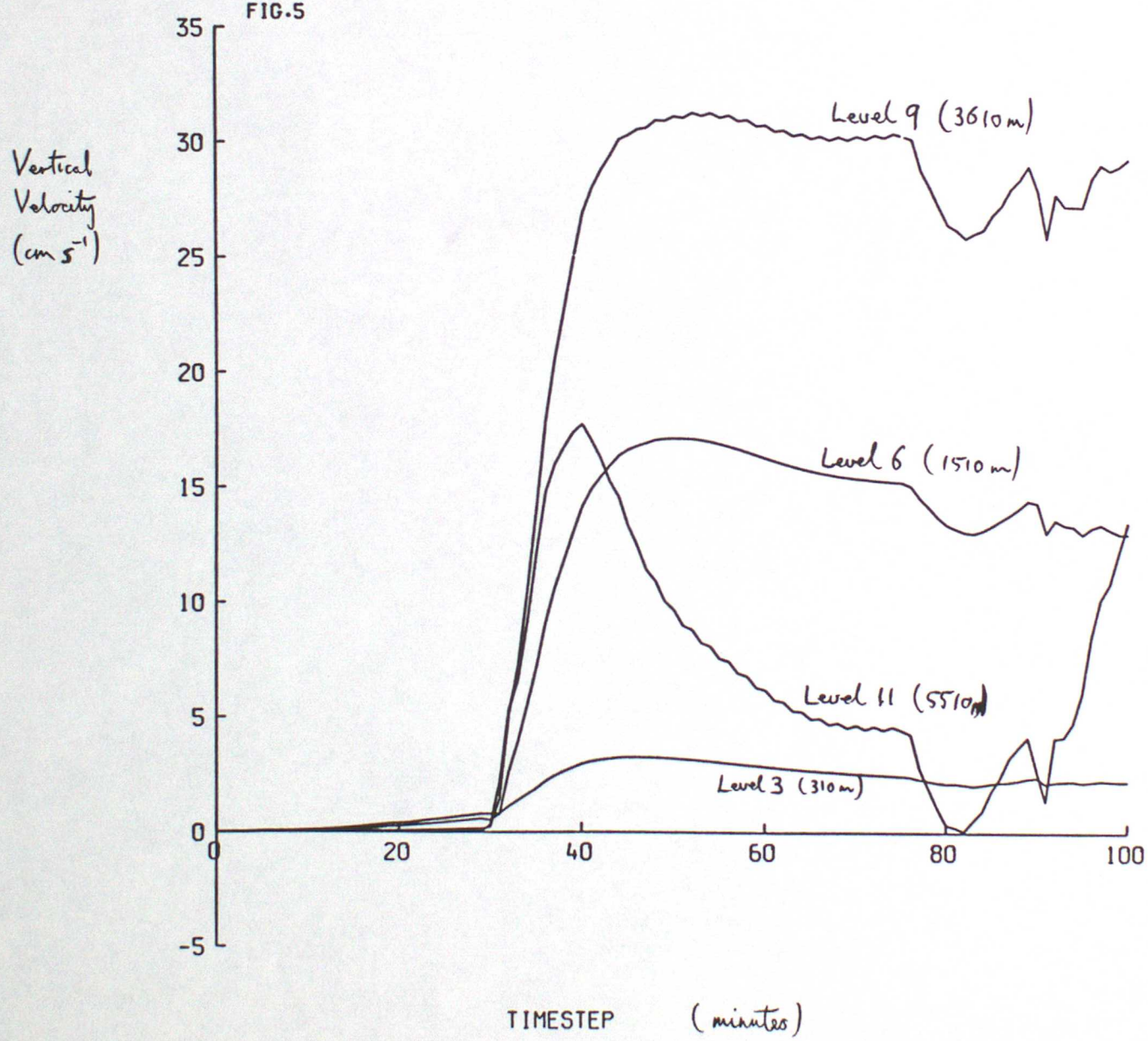
Vertical Velocity (cm s⁻¹)
35
30
25
20
15
10
5
0
-5
0
20
40
60
80
100
Level 9 (3610 m)
Level 6 (1510 m)
Level 11 (5510 m)
Level 3 (310 m)
TIMESTEP (minutes)

Fig. 5

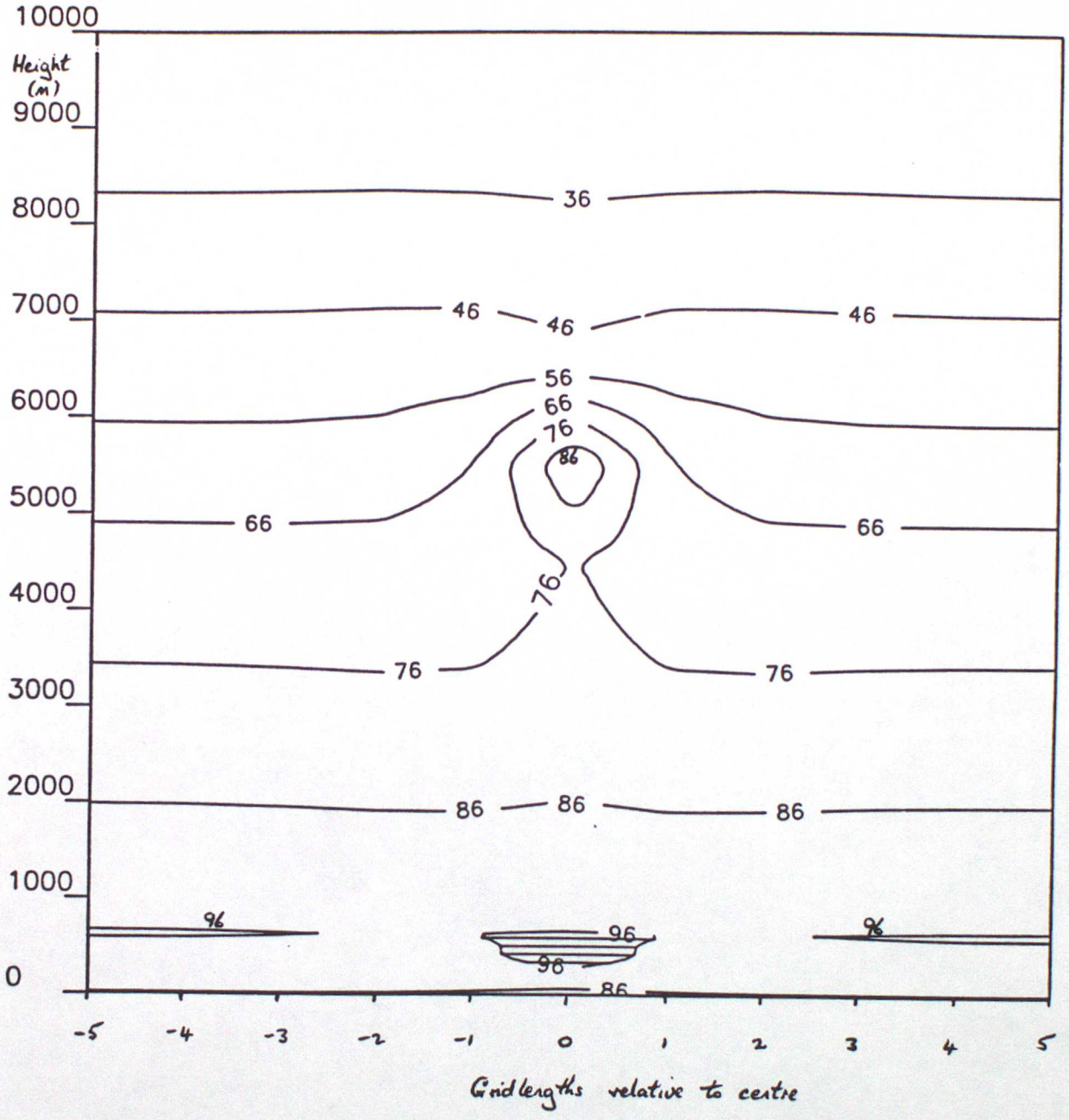
10000
Height (m)
9000
8000
7000
6000
5000
4000
3000
2000
1000
0
36
46
46
46
56
66
76
86
66
66
76
76
76
86
86
86
96
96
96
96
86
-5
-4
-3
-2
-1
0
1
2
3
4
5
Grid lengths relative to centre

Fig. 6

FIG.7

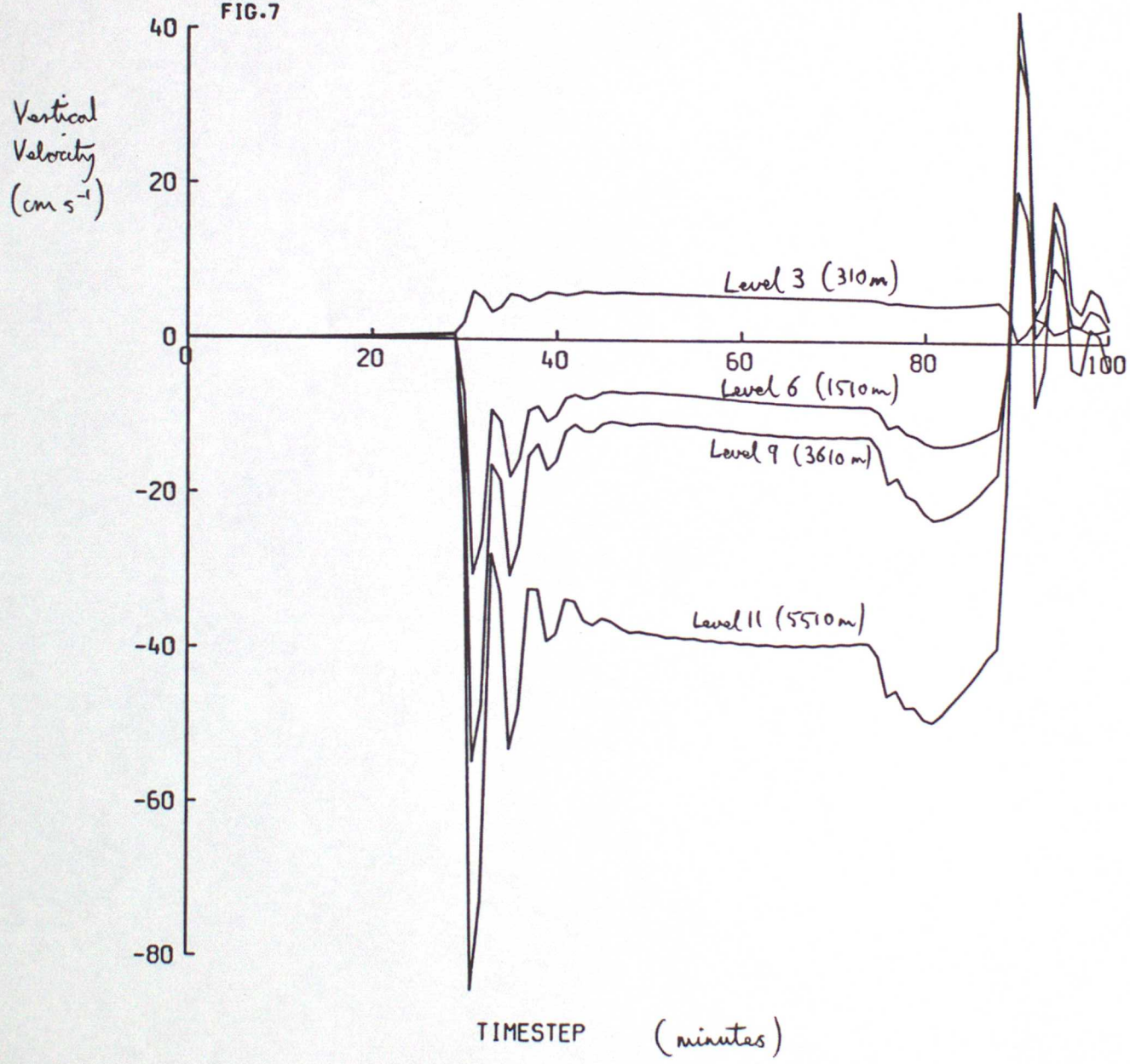
Vertical Velocity (cm s⁻¹)
40
20
0
-20
-40
-60
-80
0
20
40
60
80
100
Level 3 (310m)
Level 6 (1510m)
Level 9 (3610m)
Level 11 (5510m)
TIMESTEP (minutes)

Fig-7

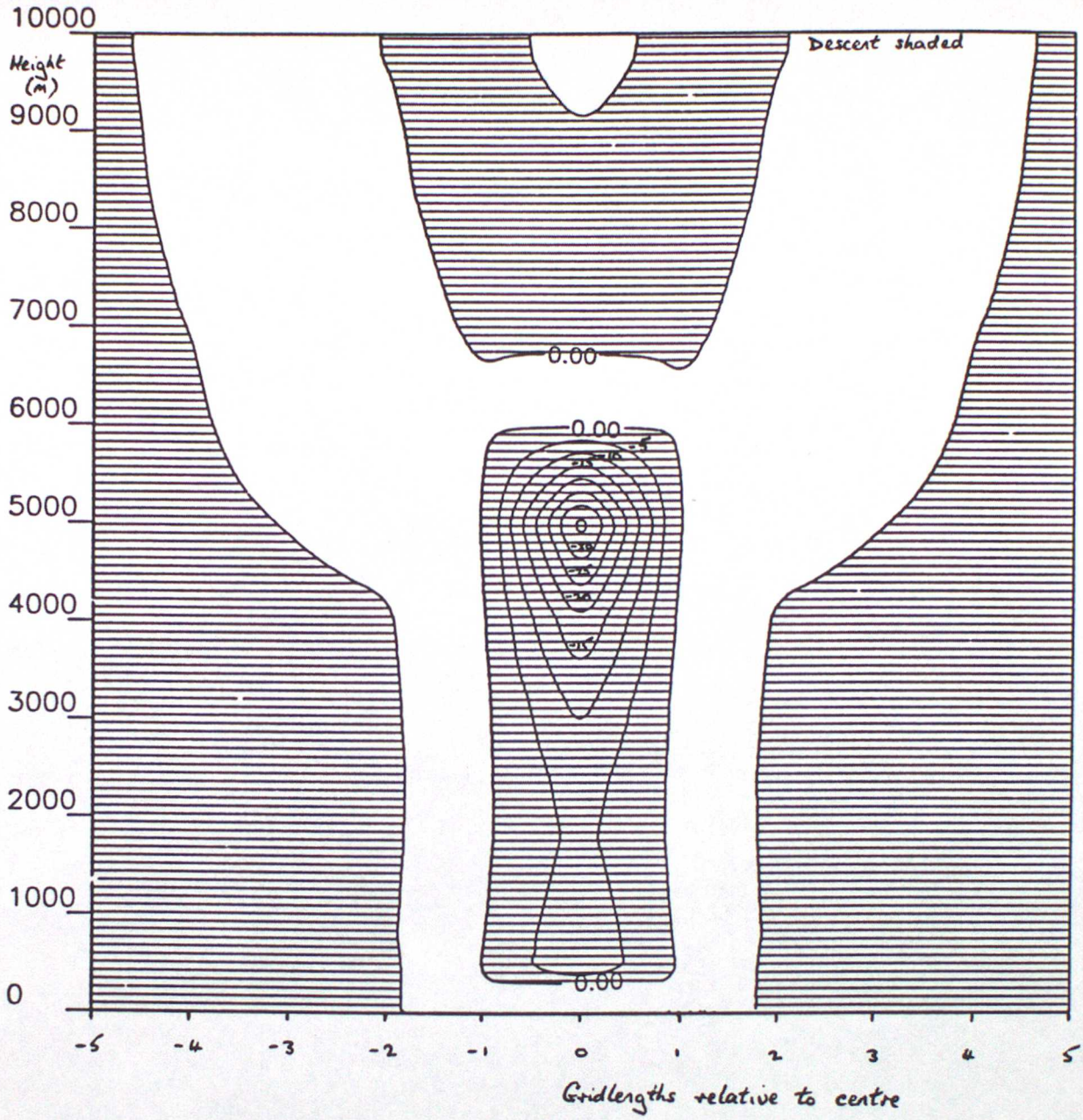
10000
Height (m)
9000
8000
7000
6000
5000
4000
3000
2000
1000
0
Descent shaded
0.00
0.00
0.00
-5
-10
-15
-20
-25
-30
-35
-5
-4
-3
-2
-1
0
1
2
3
4
5
Gridlengths relative to centre

Fig. 8

FIG.9

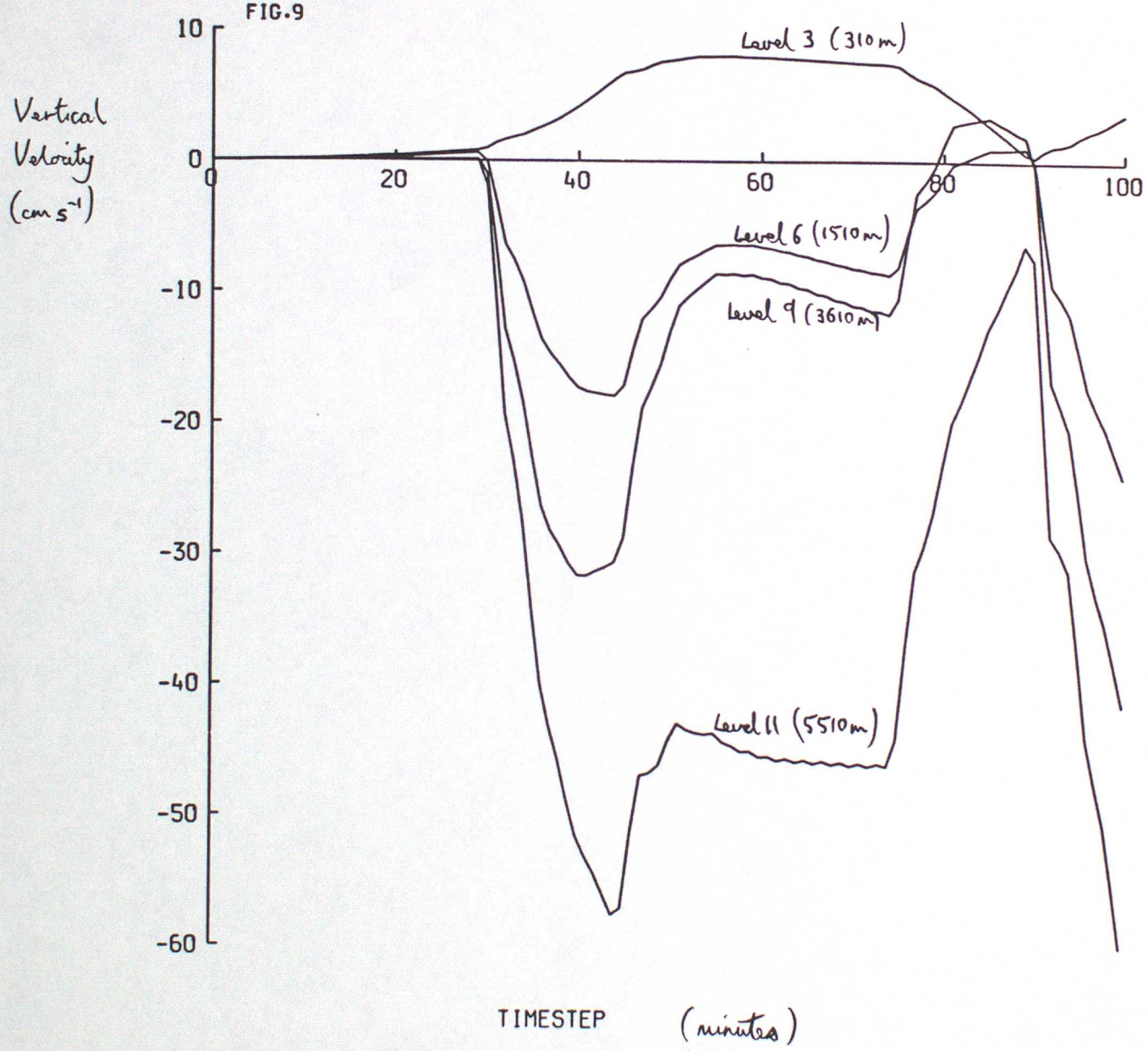
Vertical Velocity (cm s⁻¹)
10
0
-10
-20
-30
-40
-50
-60
0
20
40
60
80
100
Level 3 (310m)
Level 6 (1510m)
Level 9 (3610m)
Level 11 (5510m)
TIMESTEP (minutes)

Fig. 9.

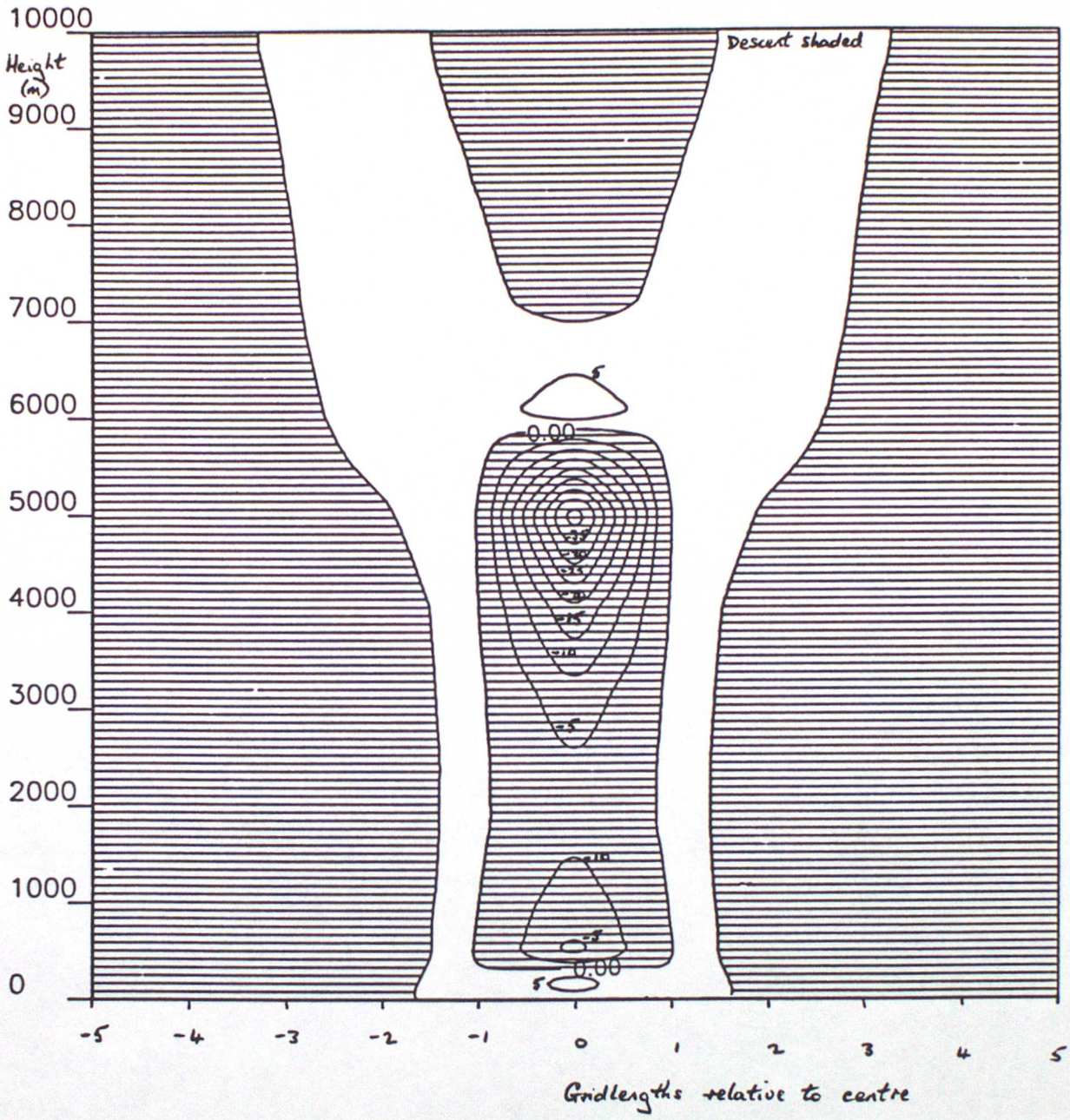
10000
Height (m)
9000
8000
7000
6000
5000
4000
3000
2000
1000
0
Descent shaded
5
0.00
-5
-10
-15
-20
-25
-30
-10
-5
0.00
5
-5
-4
-3
-2
-1
0
1
2
3
4
5
Gridlengths relative to centre

Fig. 10

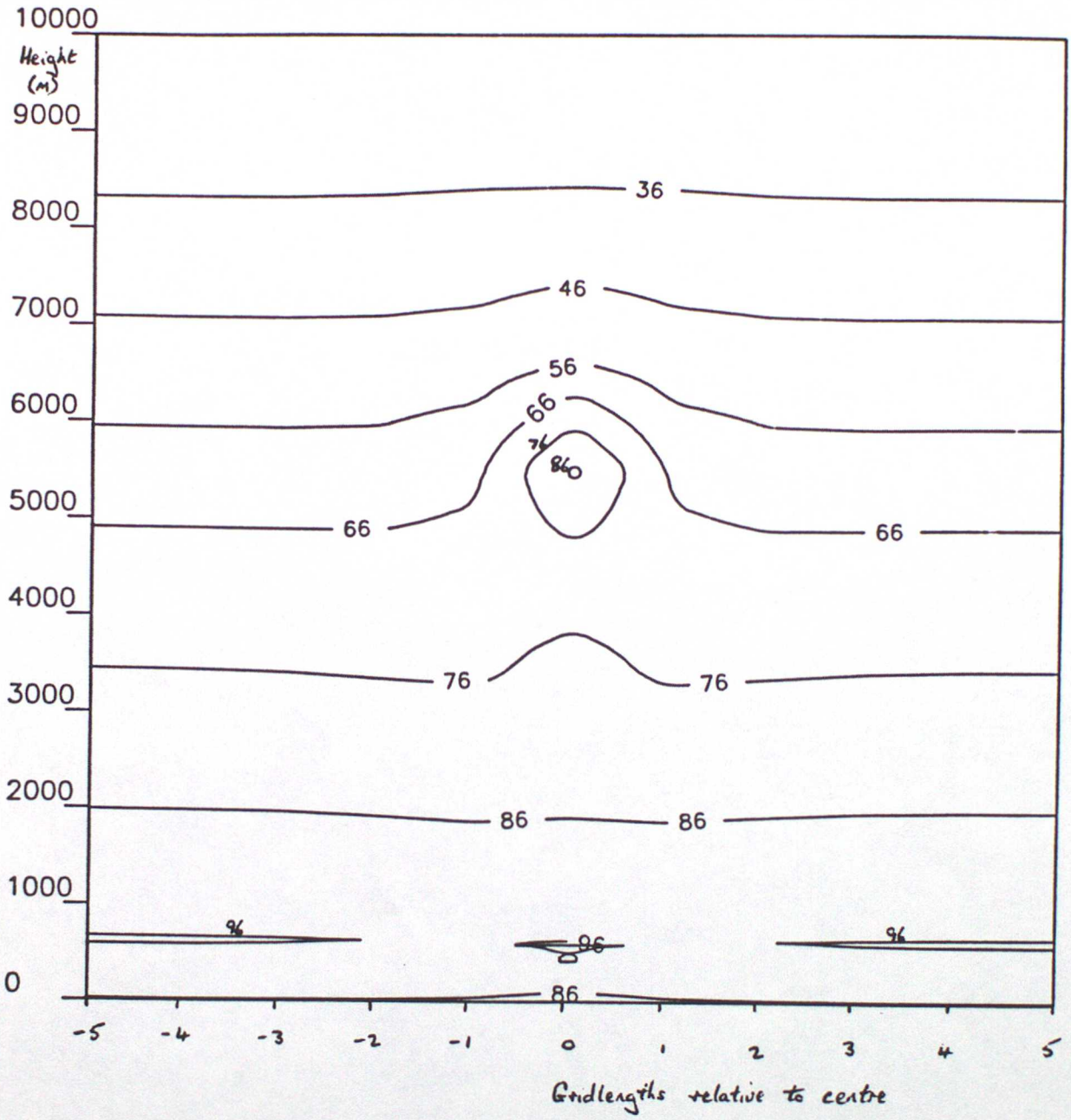
10000
Height (m)
9000
8000
7000
6000
5000
4000
3000
2000
1000
0
36
46
56
66
76
86
66
66
76
76
86
86
96
96
96
86
-5
-4
-3
-2
-1
0
1
2
3
4
5
Gridlengths relative to centre

Fig. 11

FIG.12

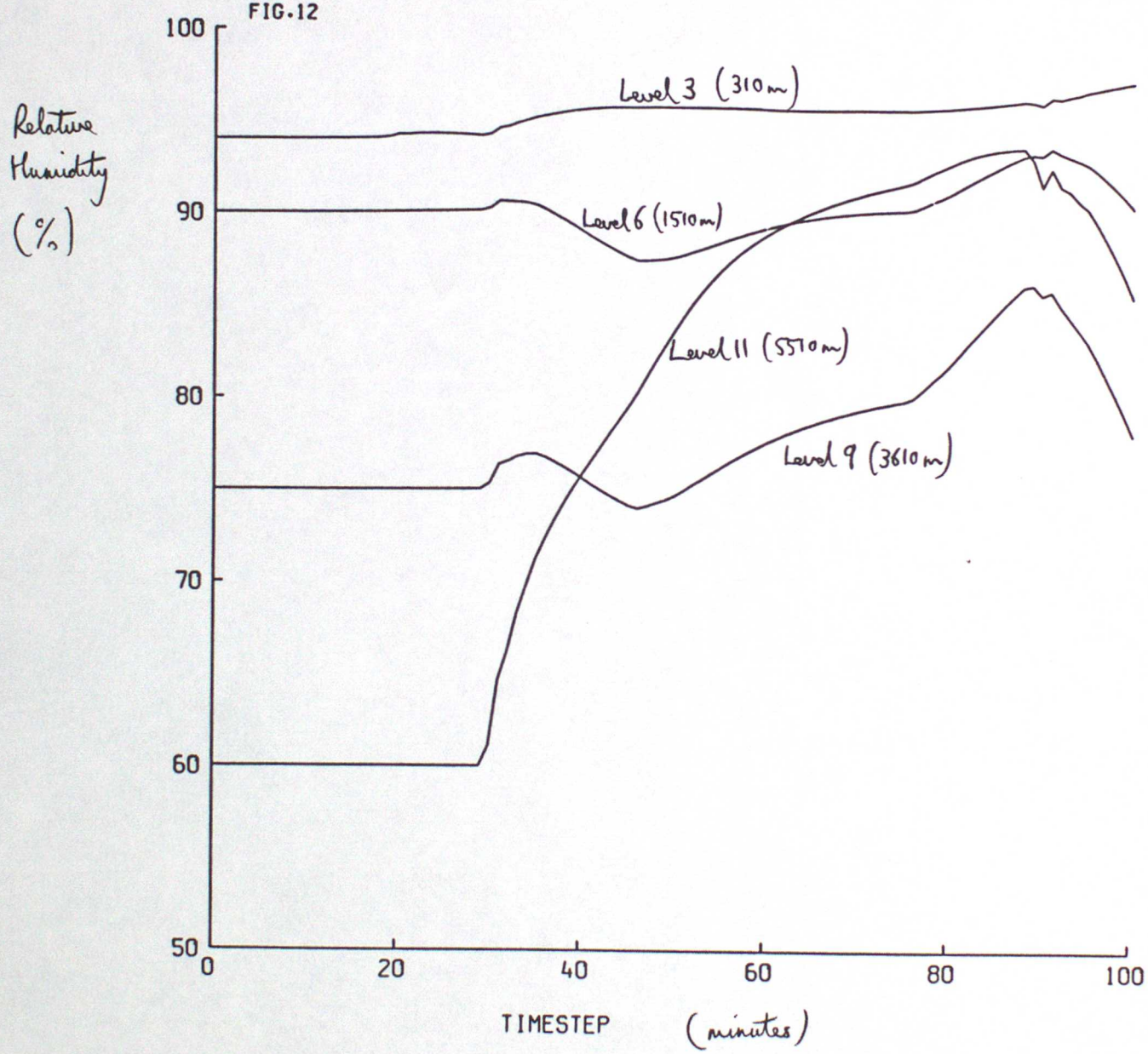
Relative Humidity (%)
100
90
80
70
60
50
Level 3 (310m)
Level 6 (1510m)
Level 11 (5510m)
Level 9 (3610m)
0
20
40
60
80
100
TIMESTEP (minutes)

Fig.12

FIG.13

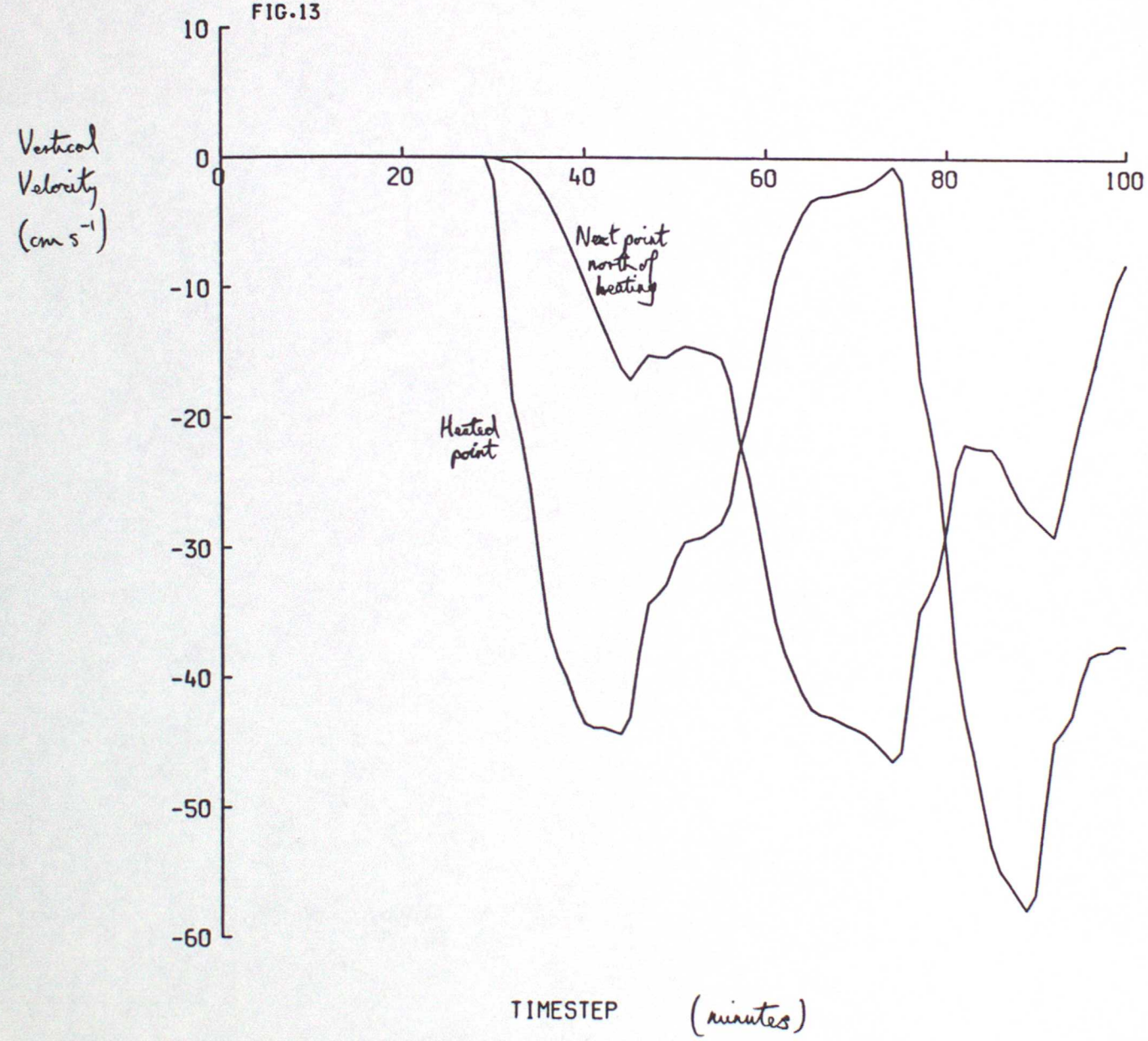
Vertical Velocity (cm s⁻¹)
10
0
-10
-20
-30
-40
-50
-60
0
20
40
60
80
100
Next point north of heating
Heated point
TIMESTEP (minutes)

Fig. 13.

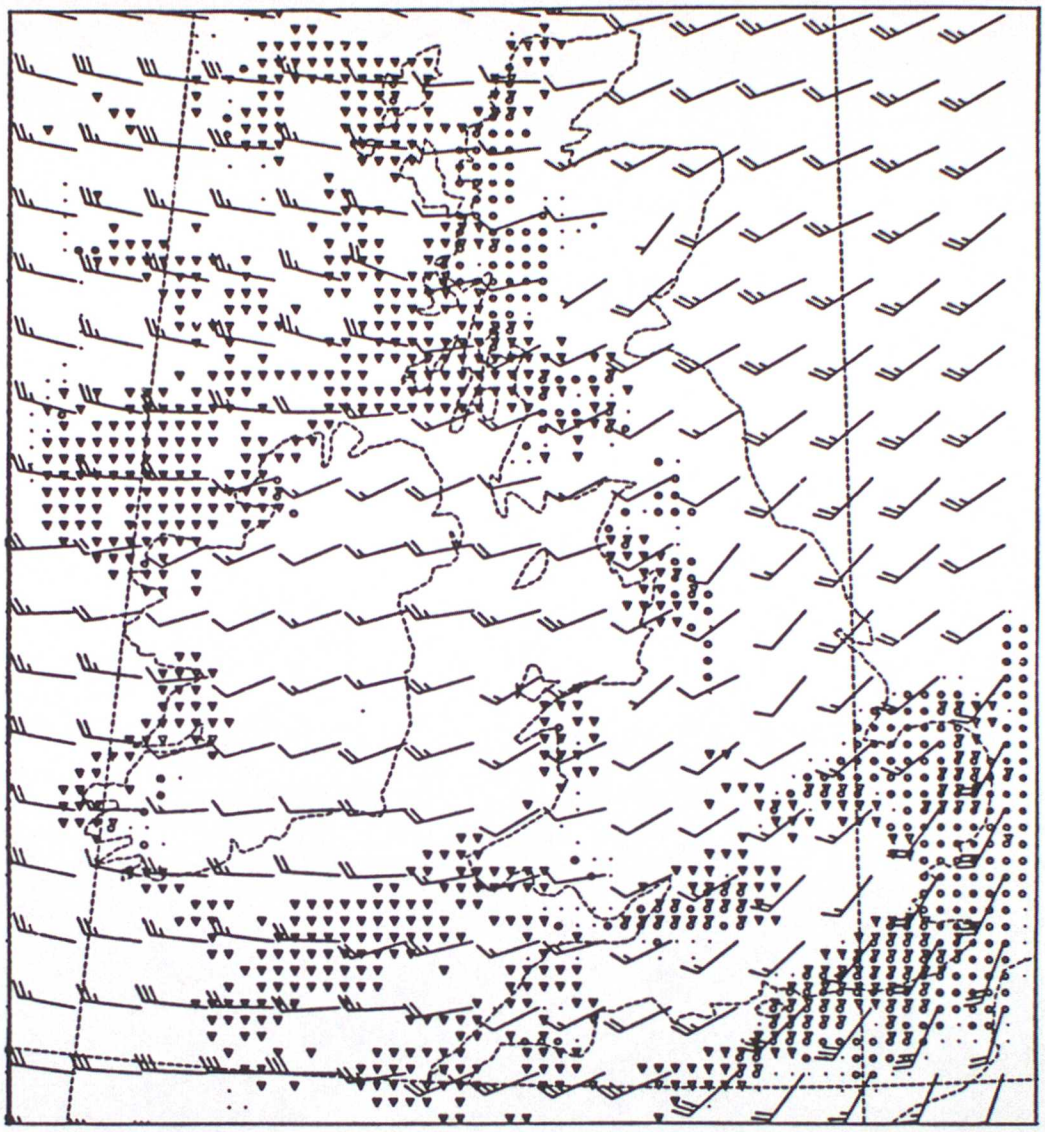

Fig. 14

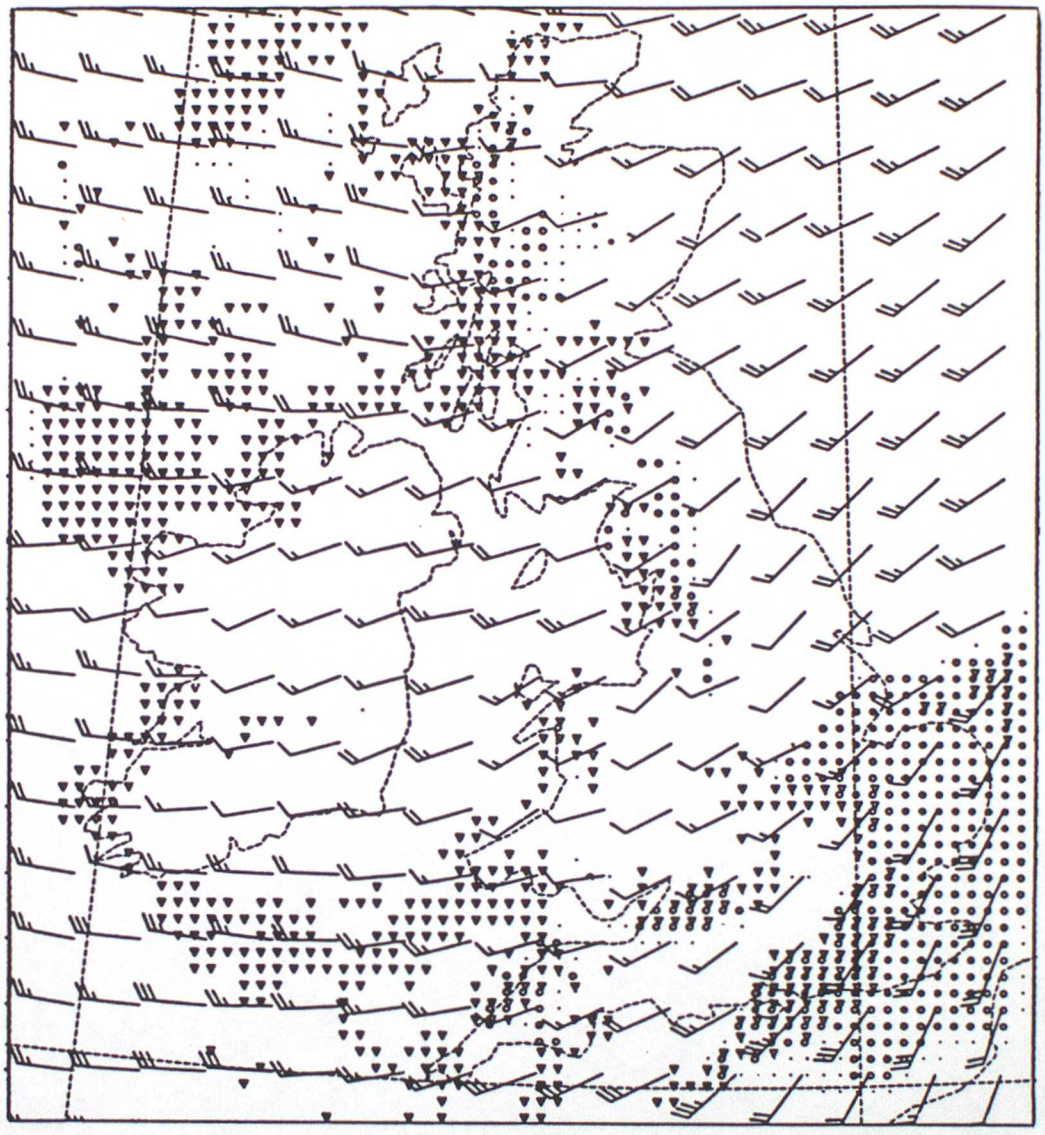

Fig. 15